Journal of Cardiovascular Disease Research

ISSN: 0975-3583, 0976-2833 VOL14, ISSUE 08, 2023

FORMULATION AND DEVELOPMENT OF ANTITUBERCULAR DRUG LOADED NANOPARTICLE FOR THE TREATMENT OF TUBERCULOSIS

[1]Yashwant Singh, [2]Ritika Singh, [3]Dhirendra Pratap Singh, [4]Mark Masih, [5]Shabenoor Siddiqui

[1] Research Scholar, Lords University, Alwar, Rajasthan

[2] Research Scholar, SMAS, Galgotias University, Greater Noida

[3] Research Scholar, SAGE University, Bhopal

[4] Lecturer, Nand Kishore College of Pharmacy, Prayagraj

[5] Scholar, United Institute of Pharmacy, Allahabad, U.P

ABSTRACT-

Multidrug-resistant TB is on the rise, which has brought to light both the need for the creation of novel TB drug therapies and the drawbacks of the present conventional TB treatment, particularly the extended duration of the treatments and the difficulties with patient compliance. In order to cure tuberculosis, the current work's objective was to produce gelatin nanoparticles carrying rifabutin. In this study, rifabutin-loaded gelatin nanoparticles (GNP) were created as a delivery system using a double desolation process. The resultant NPs were evaluated for particle size, surface charge, particle morphology, percentage of drug entrapment, in-vitro drug release research, stability studies, and *ex vivo* studies. The average particle size of mannosidase GPs was 373 potentials has been recorded at 11.46±0.26mV. Percent drug loading was found to be 52.4±1.68 which was lesser than RIF loaded GNPs. The *in vitro* drug release profiles of RIF-loaded GNPs and MN-GNPs were studied using a dialysis membrane. The GNP formulation showed 94.2±6.38% drug release in 120 hours, whereas the MN-GNPs showed 84.64±5.76% RIF release at the end of 120 hours. Drug delivery method containing rifabutin gelatin nanoparticles may show to be a promising route toward the creation of an efficient TB therapy.

Keywords: Rifabutin Polymeric Nanoparticles, gelatin nanoparticles (GNP), Tuberculosis, Targeted drug delivery

1. INTRODUCTION-

Mycobacterium tuberculosis, which causes TB, is a chronic infectious illness that has infected over a billion people globally. One-fourth of all TB cases worldwide are recorded each year, and India is the

ISSN: 0975-3583, 0976-2833 VOL14, ISSUE 08, 2023

second-most populous country in the world. [1] According to the World Health Organization's (WHO) Global Tuberculosis Report 2021, there are an estimated 9.9 to 11 million new cases of TB worldwide each year, with 1.6 million deaths. [2] In the nation most severely impacted by AIDS, the incidence of TB has increased significantly as a result of HIV-1 infection. The first-line antitubercular medicines (ATDs) Rifampicin (RIF), Isoniazid (INH), and Pyrazinamide (PYZ) were employed for cuthe rrent frontline treatment of tuberculosis. For oral administration in the initial phase, three doses of INH, RIF, and PYZ per week for two months was indicated by the specifically observed short course of treatment (DOTS).These first-line antitubercular medications have a number of drawbacks, including drug resistance, liver damage, gastrointestinal problems, rashes, etc. [3] The growth omultidrug-resistantnt TB has highlighted both the necessity for the development of novel TB drug therapies and the shortcomings of the current conventional TB treatment, especially the lengthy duration of the treatments and the issues with patient compliance.[4] This made formulation scientists more motivated to create nano-particulate delivery systems for better disease control.

Rifabutin (RFB), also known as the M. avium-intracellular complex (MAC), has activity against mycobacteria, including atypical species like Mycobacterium avium and Mycobacterium intracellular. It serves as a substitute for macrolides and is generally more effective than rifampicin in vitro against isolates of Mycobacterium TB that are susceptible to that drug. It is also used to prevent MAC infection in individuals with immune system deficiencies. [5]

Nanoparticles (NPs) are solid dispersions or particles with a size between 10 and 1000 nm. The medication is broken down, trapped, encapsulated, or bound using a nanoparticle matrix. A variety of alternative preparation methods can be used to create nanoparticles, nanospheres, and nano capsules. [6] In contrast, nanospheres are matrix systems where the drug is physically and evenly distributed, and nano capsules are systems where the medication is contained within a hollow encircled by a special polymer membrane. Biodegradable polymeric nanoparticles coated with hydrophilic polymers like poly (ethylene glycol) (PEG), also known as long-circulating particles, have been used as potential drug delivery devices in recent years due to their capacity to circulate for an extended period of time, target a specific organ, carry DNA in gene therapy, and deliver proteins, peptides, and genes. [7-8]

The main goals in developing nanoparticles as a delivery system are to regulate particle size, surface properties, and release of pharmacologically active compounds in order to achieve the desired site-specific effect of the medication at the therapeutically suitable rate and dosing regimen. Through an

ISSN: 0975-3583, 0976-2833 VOL14, ISSUE 08, 2023

increase in therapeutic potency and effectiveness, nanoparticles showed tremendous potential. NPs are thought to deliver drugs more effectively than microparticles. The selectivity of NPs towards target locations is increased by chemically modifying their surfaces with specialized recognition ligands, functional groups, and polymers of different sizes and charges. [(9)] Drug or other bioactive substance solubility, bioavailability, and bioactivity are improved when they are enclosed in NPs. A few NP types that have significantly enhanced cellular trafficking and the transport of therapeutic genes and drugs to their designated regions of action include micelles, liposomes, and polymeric systems. [(10)] Several studies have shown that nanoparticle encapsulation of TB drugs can increase their effect compared to free-administered drugs. [(11)] This can potentially dramatically increase the effect of the therapy and reduce the dosing frequency.

Nanoparticles can be a helpful strategy for treating tuberculosis (TB) in two different ways: (i) for their inherent antimycobacterial activity; and (ii) as vehicles for well-known antitubercular drugs to reduce dosage and drug-associated side effects and allow administration via convenient administration routes like pulmonary or oral ones. A wide range of nanocarriers, including polymeric nanoparticles, nano capsules, micelles, dendrimers, nanogels, and liposome, have been designed to access the reservoirs of Mtb. By physical encapsulation, adsorption, or chemical conjugation, therapeutic agents can be added to nanocarriers. Another significant benefit of employing nanocarriers is the ability to actively or passively target host cells. [(12-13)] Polymers have attracted a lot of attention in the drug delivery field over the past few decades because they provide a variety of appealing qualities. Due to a number of important characteristics, polymeric NPs are perfect for delivering antimicrobial medications. [(14-15)] PNPs have been created using a variety of biocompatible and biodegradable natural and synthetic polymers. Due to their biodegradability, these polymers are broken down into individual monomers inside the body and eliminated by regular metabolic processes. [(16)]

Since pulmonary TB is the most common type, an exciting alternative to the oral route is inhaled TB therapy employing specialized drug delivery devices. Delivery of pulmonary medications has drawn a lot of interest recently due to its benefits. Inhalation delivers drugs directly to the site of action with fewer systemic side effects than oral administration. Because the drugs are delivered directly to the lungs, the infection's main location has a higher drug concentration. Due to the lung's enormous surface area, high blood flow, and unusually thin alveolar-capillary membrane, the drugs are quickly absorbed.

ISSN: 0975-3583, 0976-2833 VOL14, ISSUE 08, 2023

As a result, less medication is needed than would otherwise be the case. [17] A practical method for creating a respiratory adjuvant to oral TB medicine is enabled by nanotechnology. [18]

Numerous polymers have been used in drug delivery studies because they can efficiently carry the drug to a target region, increasing the therapeutic benefit while reducing side effects. Gelatin is the most well-known category of materials for controlled release. Patient comfort, increased effectiveness, and reduced toxicity of current drugs are benefits of controlled drug delivery systems over conventional techniques. The ability gelatin nanoparticles to lessen the toxicity associated with the majority of medications makes them one of the most promising options for regulated pharmaceutical release. The biocompatible polymers that makeup gelatin is produced from the collagen that is present in animal skin and bones. [19] Therefore, the goal of the current work was to create gelatin nanoparticles containing rifabutin for the treatment of TB.[19,20]

2. Material and methods-

2.1 Material- the Rifabutin was obtained from Lupin Ltd., Pune, and Gelatin were purchased from S D Fine Chem Ltd., Indore. The other solvents and chemicals were purchased from Rankem (Sugandha Enterprises PaontaShahib), H.P., and S D Fine Chem. Ltd., Bhopal, India.

2.2 Methods-

2.2.1 Preformulating studies- To assure the creation of a stable dosage form that is also therapeutically efficacious and safe, preformulation studies are required. Rifabutin was used in this investigation to identify the drug. A little amount of the drug powder was placed on butter paper and examined in an area with adequate illumination. Rifabutin's melting point was then determined using a melting point equipment (Tempo, Mumbai). FTIR Spectroscopy was used to establish the drug's excipient compatibility study. Lansoprazole estimation was carried out using UV-Visible Spectrophotometry. For the quantitative assessment of the medication, a spectrophotometric calibration curve was created based on UV absorption at a maximum wavelength of 275 nm in PBS pH 6.8. The sample was qualitatively tested for its solubility in various solvents and the partition behavior of drug was examined in n-octanol: water, n-octanol: PBS (7.4) system.

2.2.2 Formulation of gelatin nanoparticles (GNPs) –

ISSN: 0975-3583, 0976-2833 VOL14, ISSUE 08, 2023

In order to create nanoparticles, double desolvation was used. In 10 ml of water, 0.2 gm (2.0%) of gelatin was dissolved by keeping the temperature at 401°C. The high molecular mass (HMM) gelatin was then precipitated by adding 10 ml of acetone as a desolvating agent to 10 ml of gelatin solution. After discarding the supernatant, the HMM was once again dissolved in 10 ml of distilled water while being constantly stirred at 1200 rpm. With the aid of HCL, the pH of the solution was then adjusted to 3.0. The medicine solution, which was 0.1% w/w, was then added. By adding acetone drop by drop and stirring for 30 minutes at 1200 rpm with a magnetic stirrer, the gelatin was re-desorbed. The developed gelatin nanoparticles were cross-linked with 200µl of room-temperature aqueous glutaraldehyde solution (25%, v/v), while being agitated at 1200 rpm for 12 hours. We first used cysteine to neutralize the excess before sonicating the gulteraldehyde-free nanoparticles for 2.0 minutes. The particles were cleaned after centrifugation at 10,000 rpm for 20 minutes, and the cleaned nanoparticles were kept cool.

Optimization of formulations: Gelatin and glutaraldehyde concentration were optimized. In order to achieve nanometric size, low polydispersity index (PDI), and maximum drug entrapment effectiveness, the effects of these factors were observed. Table-1 lists various formulation variables along with their formulation codes.

Table 1: Formulation composition of various Rifabutin-loaded gelatin nanoparticles (Type A- 300 Bloom Strength).

S. No.	Formulation code	Variables	Values
1.	GNP 1	Volume of crosslinking agent (gluteraldehyde)	50 µl
	GNP 2		100 µl
	GNP 3		200 µl
	GNP 4		300 µl
	GNP 5		400 µl
	GNP 6		500 µl
2.	GNP 1	Gelatin Concentration	1%
	GNP 2		2%
	GNP 3		4%
	GNP 4		8%

2.2.3 Characterization of nanoparticles

The prepared gelatin nanoparticles were characterized for Particle size, Surface charge, Particle Morphology, Surface Morphology, % Drug entrapment, and *In-vitro* Drug Release study. Using a Zetasizer (DTS Ver. 4.10, Malvern Instruments, England), photon correlation spectroscopy was utilized to determine the average particle size and polydispersity index of the GNPs. Using laser Doppler

ISSN: 0975-3583, 0976-2833 VOL14, ISSUE 08, 2023

anemometry and a Malvern Zetasizer (also known as a Doppler Electrophoretic Light Scatter Analyzer), the zeta potential of the nanoparticles was assessed. To see the particle morphology, a transmission electron microscope (TEM) was employed. At MANIT, Bhopal, a scanning electron microscope (SEM) was used to analyze the surface morphology. A Sephadex micro-column was used to determine the amount of drug entrapment. Using a dialysis tube, it was possible to measure the in vitro drug release of the GNPs formulation's trapped rifabutin.

2.2.4 Stability studies

To find out whether drugs leached from gelatin during storage, a physical stability test was conducted. The samples were kept in glass vials and held for a month at two different temperatures, namely room temperature (250C) and refrigerated temperature (4-80C), with samples being taken at regular intervals. By evaluating the formulations' encapsulation effectiveness, the drug leakage from those formulations was examined.

2.2.5 Ex-vivo studies

Cellular uptake of fluorescein isothiocyanates (FITC) loaded GNPs: Macrophage cell lines J774 was used for the cellular uptake study. The uptake study was performed at 1-, 2- and 6-hour intervals.

MTT cytotoxicity assay: 774 cells were resuspended in new growth media at a concentration of 1X103 cells/ml. By using a 3- (4-5 dimethylthiazol-2H)-2, 5-diphenyl tetrazolium bromide (MTT) (Sigma Aldrich) colorimetric assay, the materials' capacity to suppress cell growth was assessed.

Hemolytic Toxicity: The study was carried out on whole human blood, which was collected in Hi-Anticlot vials (Himedia, India). The degree of hemolysis was determined by the following equation:

$$\text{Hemolysis (\%)} = Abs - Abso\ /Abs100 - Abso \text{ X } 100$$

where Abs, Abs100, and Abso are the absorbances of the sample, solution of 100% hemolysis, and solution of 0% hemolysis; respectively.

3. Results-

3.1 Preformulation studies: Preformulation research aimed to create a database of knowledge on the pharmacological substance. In order to create a formulation for nanoparticles, this information would be useful.

ISSN: 0975-3583, 0976-2833 VOL14, ISSUE 08, 2023

***Identification of Drug*:** Identification studies showed that the drug supplied by Lupin Pharma Pvt.Ltd, Pune matched with the official standard as prescribed (Table 2).

Table 2: Physical identification tests of Rifabutin

Parameters	Rifabutin (RIF)	Results
Appearance	Red-violet, crystalline,hygroscopic powder	Complies
Odor	Odorless	Complies

The melting point of the drug: A capillary melting point method was used to determine the melting point of the drug. It was observed that the melting point of Rifabutin was found to be 153 ± 2^0Csimilar to the reported value which proved that the received drug samples meet the reported properties. Any contaminant, if present, will cause the melting point of a particular medicinal compound to vary. The sample medication passed the standard test for Rifabutin, as determined by the preceding analysis.

FTIR spectroscopy of drug: FTIR spectra of Rifabutin were obtained and compared with reference IR spectra for identification and confirmation of various functional groups. Interpretation of FTIR spectra of Rifabutin suggests that the observed peak list meets with that of the reference peak list (Table 3 and Fig 1). The observation confirms that the drug obtained is pure.

FTIR analysis was performed in order to confirm the drug and excipients' interaction. The scan was examined for the existence of major drug peaks, the shifting and masking of drug peaks, and the formation of new drug peaks as a result of excipient interaction. In the spectra of the mixture of the drug and excipients, there are no peaks other than the typical peak, indicating that there is no interaction between the drug and excipient and that they are compatible.

Table 3: Important band frequencies in the FTIR spectrum of Rifabutin

S.No.	IR Absorption band cm^{-1}	Assignments
1.	3461.0	O-H stretching (Alcohol, ROH)
2.	2961.1	Aliphatic C-H stretch
3.	2821.9	C-H stretch (Carboxylic acid)
4.	1727.3	C=O stretch of aldehyde
5.	1671.2	C=O stretch (cyclic amide)
6.	1601.2	C=C stretch Benzene (aromatic)
7.	1526.6	Asymmetric ($ArNO_2$) stretch
8.	1421.2	O-H bending (Carboxylic acid)

ISSN: 0975-3583, 0976-2833 VOL14, ISSUE 08, 2023

11.	1064.9	C-N stretch (Amine)
12.	1164	C-O stretch (3 ROH)

Fig 1 FTIR spectrum of Rifabutin

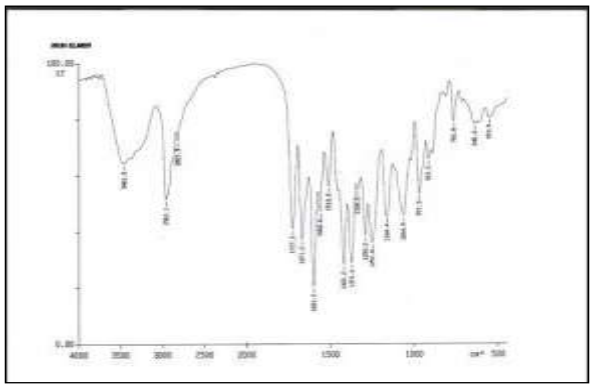

Determination of wavelength maxima (λ_{max}) and Calibration Curve of the drug: UV spectra the of drug were obtained by scanning drug solutions (10µg/ml)and showed maximum absorption at 275 nm (Fig 2).

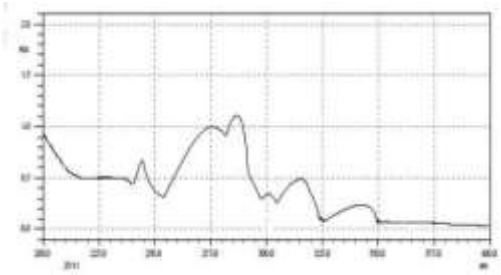

Fig. 2: UV scan of Rifabutin drug sample

The calibration curve was prepared in PBS pH 7.4 at 275nm and linearly regressed. The correlation coefficient for standard curves was found to be very near to one which indicates good co-linear correlation between concentration 2-20 µg/ml (Table 4 and Fig. 3). Hence, drugs are following Beer-Lambert Law in the above range.

Table 4-Calibration curve of Rifabutin in PBS pH 7.4

Drug concentration(mg/ml)	Absorbance	Absorbance (Regressed)	Statistical parameter

ISSN: 0975-3583, 0976-2833 VOL14, ISSUE 08, 2023

	(Observed)		
2	0.0513	0.0507	
4	0.1064	0.1011	
6	0.1509	0.1515	
8	0.1987	0.2019	
			Equation of line:
10	0.2533	0.2523	**y = 0.0252x + 0.0003**
12	0.2979	0.3027	**R^2 = 0.9991**
14	0.3567	0.3531	
16	0.3991	0.4035	
18	0.4506	0.4539	
20	**0.5129**	**0.5043**	

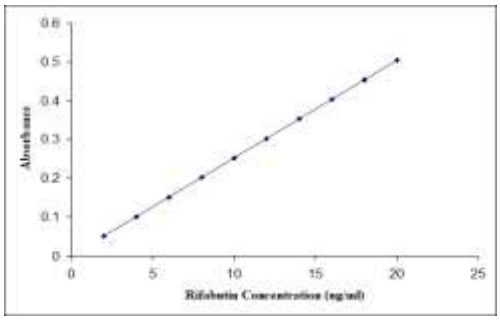

Fig. 3: Calibration curve of Rifabutinin PBS pH 7.4at 275 nm

Solubility studies

The sample was quantitatively tested for its solubility in various solvents. It was determined in solvent (i.e., water, PBS pH 7.4, methanol, ethanol, ether, chloroform etc.). Solubility profile of rifabutin is recorded in Table 5

Table 5: Solubility profile of Rifabutin

S. No.	Solvent	Solubility (mg/ml)	Solubility
1	Water	0.0092	**Insoluble**

ISSN: 0975-3583, 0976-2833 VOL14, ISSUE 08, 2023

2	PBS (pH 7.4)	0.42	**Slightly soluble**
3	Methanol	0.49	**Slightly soluble**
4	Ethanol	0.96	**Sparingly soluble**
5	Ether	0.0075	**Insoluble**
6	**Chloroform**	**55.87**	**Freely soluble**

Partition coefficient: The partition coefficient of Rifabutin was determined in n-octanol: PBS pH (7.4) system. The partition coefficient of Rifabutin was found to be 2.7 (Table 6).

Table 6 Partition coefficient of Rifabutinin n-octanol: PBS pH -7.4

Drug	**Amount of Drug (mg)**		**Partition coefficient ($Po_{/w}$)**
	Aqueous Phase	**n- Octanol**	
Rifabutin	2.76	7.24	2.7

3.2 Formulation of gelatin nanoparticles

GNPs prepared using modified two-step desolvation technique was shown to be highly stable in water and cell medium. This approach produces particles with the lowest level of aggregation and uniform dispersion. In this approach, low and variable molecular weight gelatin chains were rejected in the first desolvation stage, and high and uniform molecular weight gelatin was subsequently employed in the formation of GPs, which ensured nanometric particles with low PI.

Optimization of Concentration of glutaraldehyde

The particle size decreases steadily along with higher amounts of glutaraldehyde applied. When amount of glutaraldehyde was varied from 50-500 ML, there was approximately significant reduction in particle size from 421±6.02nm to 204±3.1nm for RIF. In contrast, the PDI (0.19±0.017) was found minimum at 300 L of glutaraldehyde. The probable reason could be that this amount was sufficient to cause uniform reduction in particles size for number of GPs formed. The EE were not significantly affected by amount of glutaraldehyde used ($p>0.05$)

ISSN: 0975-3583, 0976-2833 VOL14, ISSUE 08, 2023

(Table 7 and Fig 4 & 5).

Table 7: Optimization of Concentration of glutaraldehyde for the preparation of gelatin nanoparticles (Type- A $_{300}$)

Formulation code	Temperature	Average size(nm)	% Entrapment efficiency	Polydispersity index
GNP 1	50 µl	421±6.02	46.4±3.1	0.34±0.021
GNP 2	100 µl	367±10.1	51.2±2.4	0.22±0.034
GNP 3	200 µl	318±16.2	54.7±4.3	0.20±0.028
GNP 4	300 µl	266±13.8	59.9±3.27	0.19±0.017
GNP 5	400 µl	223±7.6	60.8±3.2	0.24±0.005
GNP 6	500 µl	204±3.1	62.4±4.8	0.37±0.041

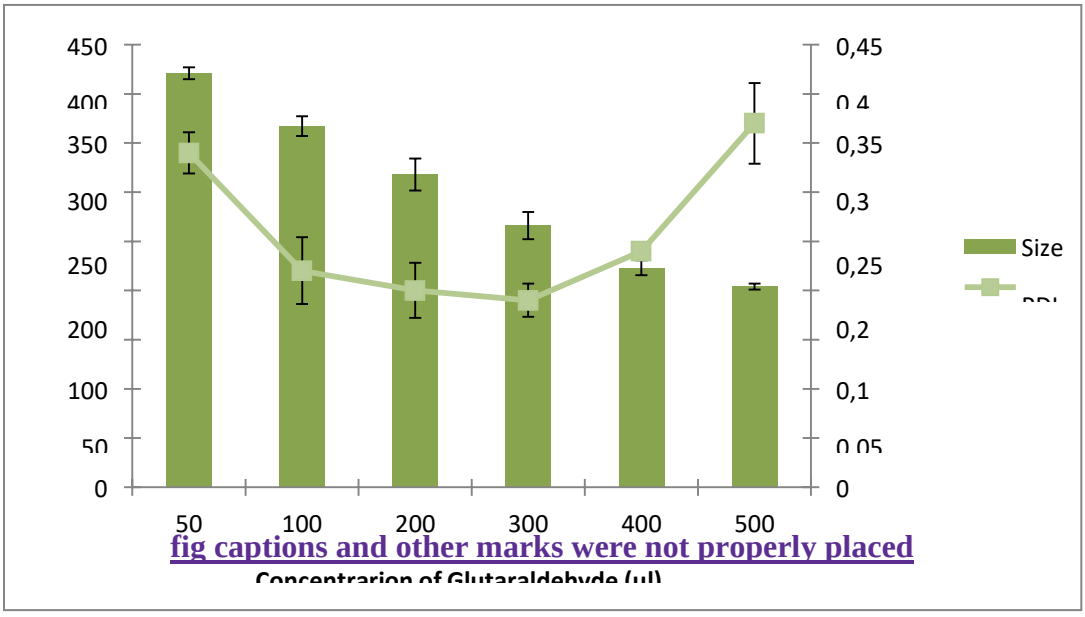

fig captions and other marks were not properly placed

Concentrarion of Glutaraldehyde (µl)

ISSN: 0975-3583, 0976-2833 VOL14, ISSUE 08, 2023

Fig 4 Effect of amount of glutaraldehyde on particle size and PDI for RIF loaded GPA_{300}

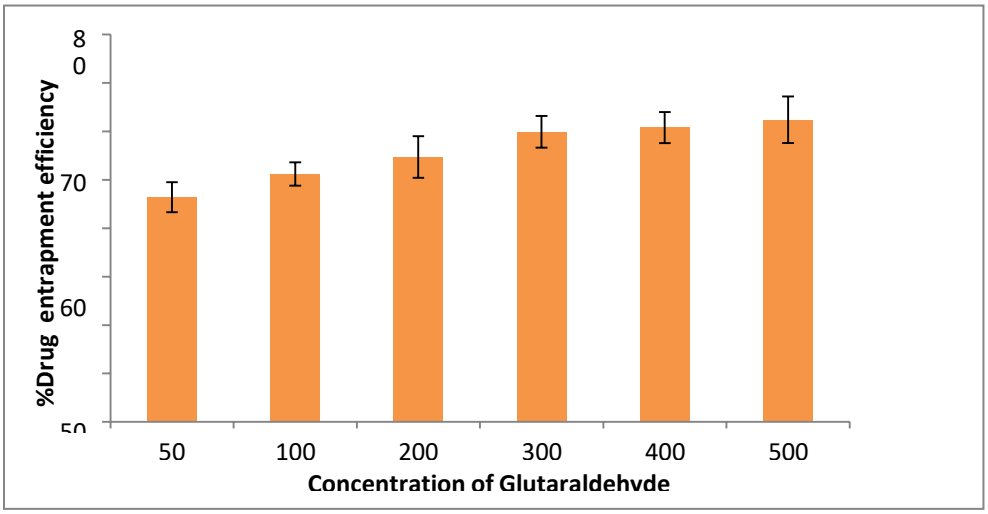

Fig 5 Effect of amount of glutaraldehyde on % EE for RIF loaded $GNPA_{300}$

Optimization of Concentration of Gelatin

The concentration of gelatin used to prepare $GNPA_{300}$ formulations was optimized on the basis of size, PDI and % EE of GNPs. The concentration of gelatin was varied from 1% to 8% w/v. The results showed that 2% w/v gelatin concentration was found to be adequate. At this concentration nanosized GNPs with good size, PDI and entrapment efficiency was obtained. On the contrary, at higher gelatin concentration (3% w/v) though spherical shaped GPs were formed but great variation in size was recorded (Table 8 and Fig 6-7).

Table 8: Optimization of Concentration of Gelatin for preparation of gelatinnanoparticles (Type- A_{300})

Formulation code	Concentration of Gelatin	Average size(nm)	% Entrapment efficiency	Polydispersity index
GNP 1	1%	192±3.5	43.2±2.4	0.14±0.013
GNP 2	2%	267±12.72	58.2±4.1	0.22±0.015
GNP 3	4%	312±12.1	60.9±6.2	0.58±0.031
GNP 4	8%	532±21.7	63.2±3.1	0.65±0.045

ISSN: 0975-3583, 0976-2833 VOL14, ISSUE 08, 2023

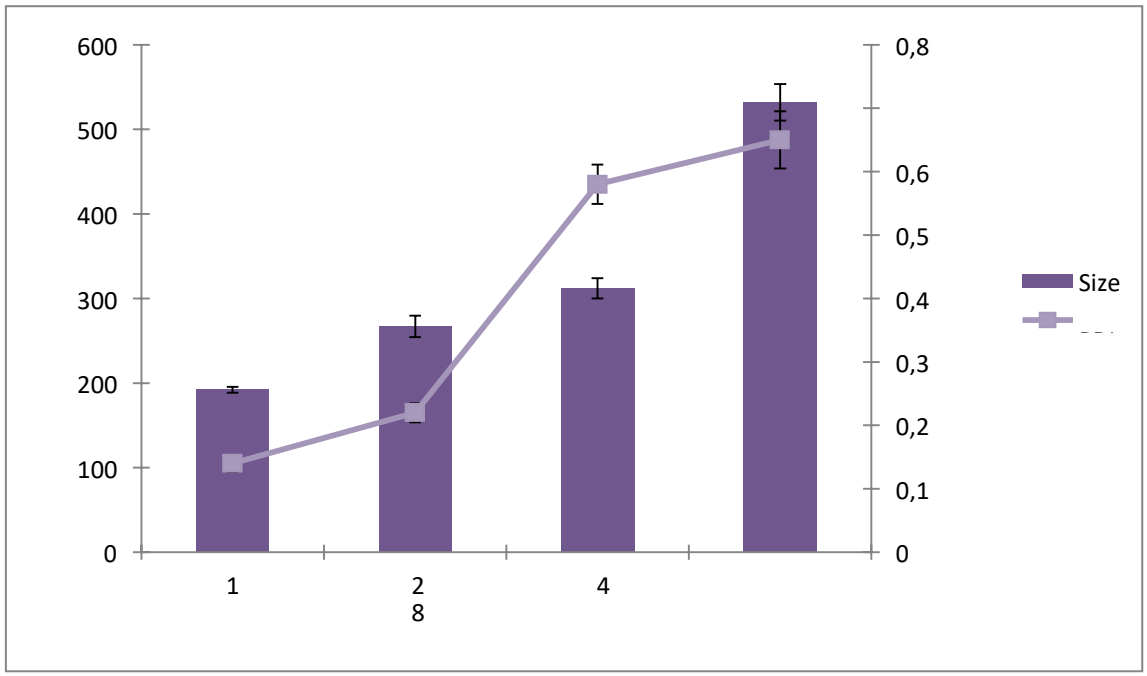

Fig 6 Effect of Concentration of Gelatin on particle size and PDI for RIF loaded GNPA$_{300}$

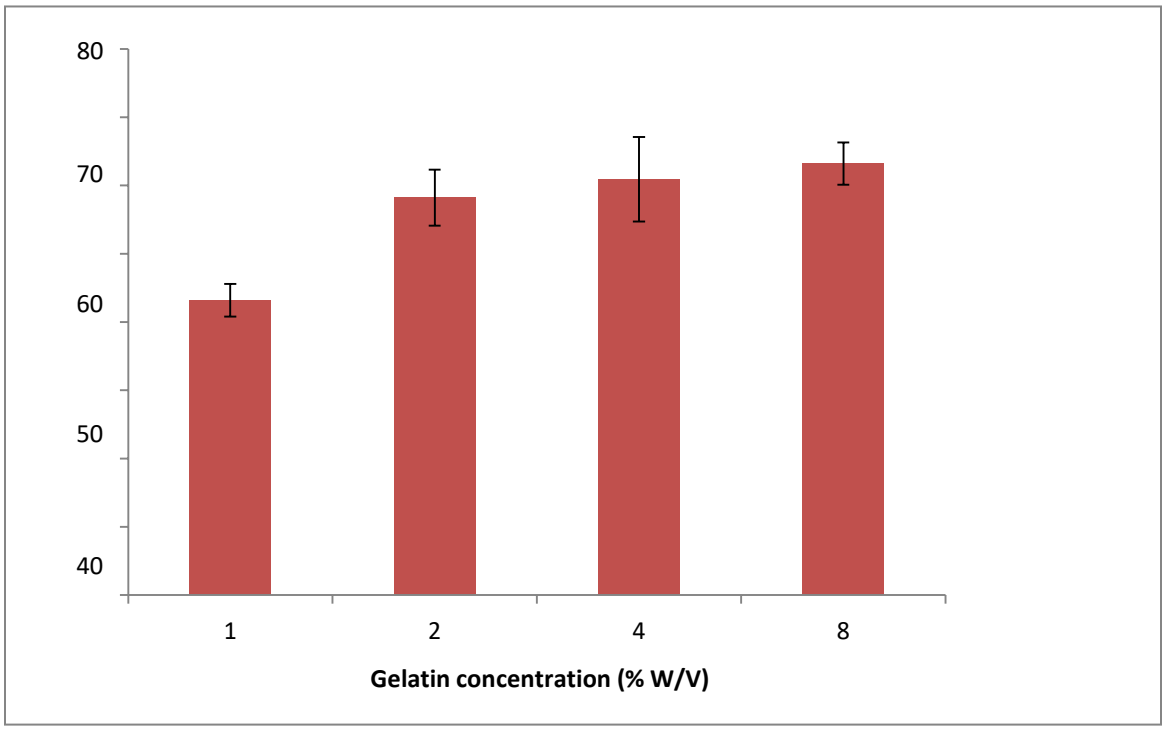

Fig 7 Effect of Concentration of Gelatin on % EE for RIF loaded GNPA$_{300}$

ISSN: 0975-3583, 0976-2833 VOL14, ISSUE 08, 2023

Mannosylation of Nanoparticles

The method involved ring opening of mannose followed by reaction of its aldehyde group with free amino groups present over the surface of prepared GPs at suitable conditions. This leads to formation of Schiff's base, and mannose became bonded over the nanoparticle surface. Using FTIR analysis, the mannosylated nanoparticles were characterised. Weak N-H stretching at 3460–3580 cm–1 and significant N-H bending at 1660 cm–1 in non-mannosylated GPs indicated the existence of primary amine groups. In the instance of MN-GNPs, the N-H bending of secondary amines at 1575 cm–1 and the C=N stretch at 1505–1465 cm–1 demonstrated the development of Schiff's base (RCH= N-R bond), showing the establishment of a connection between the mannose ligand and the amine terminal of the nanoparticles. In addition, a wide, intense, and powerful O-H stretch of mannose at 3710–3580 cm–1 and a significant C-O stretch at 1075 cm–1 demonstrated the existence of many hydroxyl groups (of mannose) in MN-GNPs (Fig 8). The various peaks of functional groups in FTIR spectra of mannosylated gelatin nanoparticles are tabulated in Table 9

Table 9 FTIR spectral illustration of MN-GNPs

Wave number (cm^{-1})	Functional group	Interpretation
3610	O–H stretch	O–H stretch of mannose
1465	C=N stretch	Amide group
1575	N-H bending	Secondary amine
2841.9	C-H bending (in plane)	Methyl and methylene group
1382.3	C-H bending (out plane)	
1075	C–O stretch	C–O stretch of carbohydrate around

Fig. 8 FTIR spectrum of mannosylated Gelatin nanoparticles (MN-GNPs)

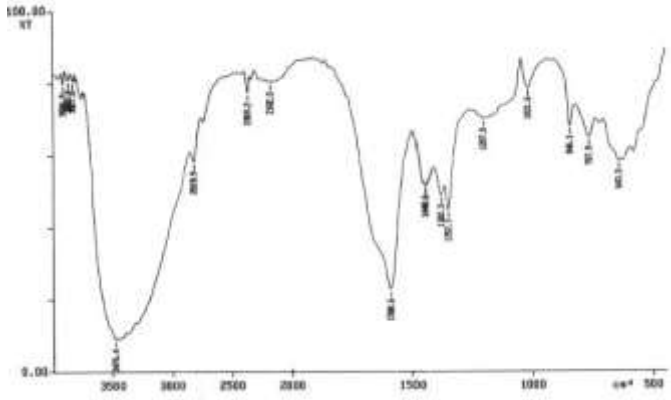

ISSN: 0975-3583, 0976-2833 VOL14, ISSUE 08, 2023

3.3 Characterization of plain and ligand coupled GNPs

Particle size and PDI

The size and PDI of various formulations prepared by gelatin A300 was observed to be 264±11.2 nm (0.241±0.011). The average particle Size of mannosylated GPs (373 □ 23 nm) was quite higher as compared to plain nanoparticles. This could be due to the anchoring of the bulky mannose molecules at the surface of the nanoparticles. The PDI data suggested that GNPs formed was monodispersed and slight increase in PDI in case of mannosylated GPs could be due to increase of the bulk of mannose on the surface of GPs (Table 10).

Surface charge (zeta potential)

The associated zeta potential of these GNPs might be used to infer their surface charge. The positive charge on the surface of gelatin can be explained to the preponderance of the NH3+ group. The high zeta potential of GNPA300 may be related to its large molecular weight and, consequently, its high amine group density at the surface. The medication loading greatly boosted the GNP's net positive. Furthermore, zeta potential is an essential indicator for the stability of GPs suspensions. A high absolute value of zeta potential for Type A gelatin suggests a significant electric charge on the surface of the drug-loaded GPs, which can cause strong repellent forces among particles to prevent aggregation of the GNPs in buffer solution. The decrease in value of zeta potential of GPs on coupling with mannose may be due to a shielding effect of ions, over the charge present at the surface of the nanoparticles. The result of zeta potential has been recorded in Table 10

Percent drug loading (w/w %)

Drug loading is an important index for novel drug delivery systems. For the entrapment efficiency study, RIF was dissolved in a predetermined amount of methanol and blended with an aqueous solution of polymer using a mechanical stirrer. The entrapment of RIF in GNPs could be explained on the basis of preferential localization of drug inside the nanoparticulate core, which was a lesser hydrophilic region as compared to outer aqueous environment and as desolvation caused removal of water from core, further allowing the better entrapment of RIF. The mannosylation of the nanoparticles has pronounced effect on the encapsulation efficiency. The mannosylation reaction involves the incubation of the nanoparticles with the sodium acetate buffer for 48 h which might

ISSN: 0975-3583, 0976-2833 VOL14, ISSUE 08, 2023

leads to the leaching of the drug to the medium and hence responsible for the lower drug entrapment as compared to the plain nanoparticles (Table 10).

Table 10 Characterization of RIF loaded Plain and Mannosylated GNPs

Formulations		Size(nm)	PDI	Drug loading (% w/w)	Actual drug loading (% w/w)	Zeta potential (mV)
GNP_{A300}	RIF	264±11.2	0.241±0.	59.5±2.82	2.3 ±0.14	15.32± 0.19
	loaded		011			
MN-GNPs	RIF	417□31.4	0.232□0.	52.4±1.68	-	11.46±0.26
	loaded		01			

TEM study

TEM was used to investigate the size and shape of nanoparticles. TEM photographssuggest that all nanoparticulate preparation were spherical in shape and in nanometric range (Fig 9 &10). However, mannosylated GPs surface was relatively less spherical and smooth incomparison to GNPs.

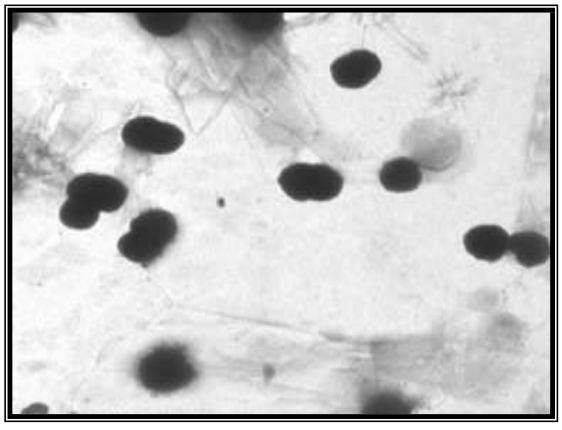

Fig 9- TEM of rifabutin loaded GNPs

ISSN: 0975-3583, 0976-2833 VOL14, ISSUE 08, 2023

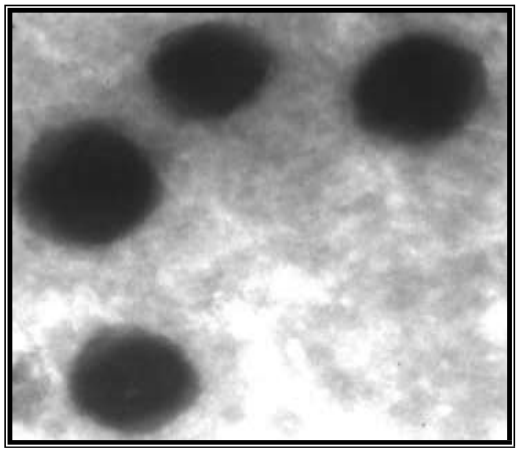

Fig 10- TEM of rifabutin-loaded mannosylated GNPs.

SEM study

The morphology of gelatin nanoparticles was determined by scanning electron microscopy (SEM). SEM analysis used to characterize the surface and morphological features of nanoparticles. It was found that the surface of GNPs was smooth and spherical (Fig 11-12).

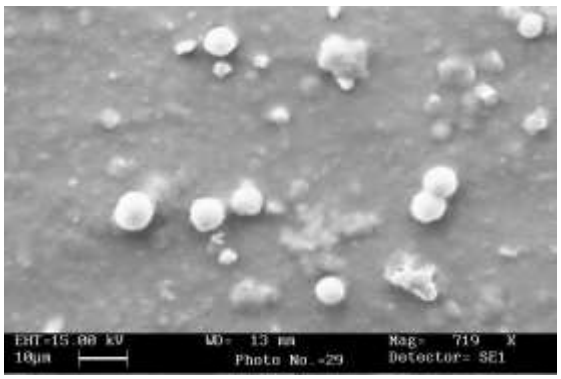

Fig 11 SEM of rifabutin loaded GNPs

ISSN: 0975-3583, 0976-2833 VOL14, ISSUE 08, 2023

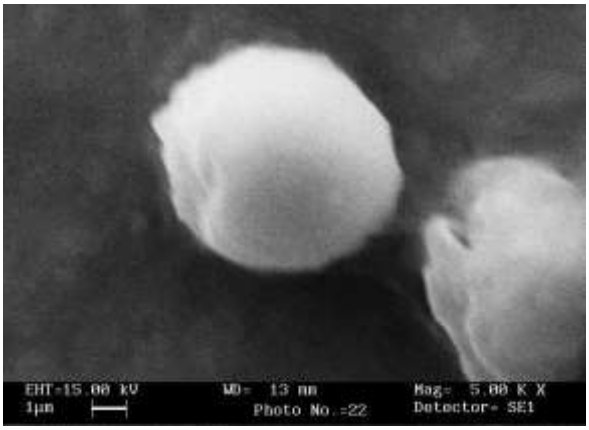

Fig 12 SEM of rifabutin-loaded mannosylated GNPs

In vitro RIF release

The in vitro drug release profiles of RIF loaded GNPs and MN-GNPs were studied using dialysis membrane and are presented in Fig 9.13. RIF's release from the gelatin matrix exhibited a biphasic pattern consisting of an early burst followed by a slower sustained release. The GNP formulation showed 94.2±6.38% drug release in 120 hours, whereas the MN-GNPs showed 84.64±5.76% RIF release at the end of 120 hours. The initial-burst drug release may be due to the release of drug present at or just beneath the surface of the nanoparticles. Slow release in the case of the MN-GNPs formulation may be attributed to the presence of the protective coat of mannose on the nanoparticle surface, which interferes with the drug release.

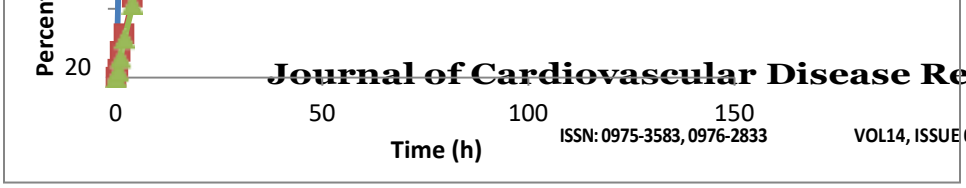

Journal of Cardiovascular Disease Research
ISSN: 0975-3583, 0976-2833 VOL14, ISSUE 08, 2023

Fig 13: *In-vitro* drug release of various RIF loaded formulations in PBS pH-7.4

3.4 Stability studies

The effects of storage time and storage temperature on residual drug content of nanoparticles were determined. After storage of formulation the percent residual drug content was determined by analyzing the amount of drug leached in the supernatant using spectrophotometric method. Samples were taken periodically and estimated for drug content (Table 11).

Table 11: Effects of temperature on % residual drug content of Nanoparticulateformulations

Formulation code	Initial	5±3° C			25±2° C		
		10 days	20 days	30 days	10 days	20 days	30 days
GNP	100	99.5±3.8	98.4±3.2	97.8±1.8	98.7±1.4	98.1±1.3	97.2±2.2
MN-GNPs	100	99.1±4.2	97.8±2.5	96.9±2.1	98.5±1.6	97.9±1.6	96.8±2.3

ISSN: 0975-3583, 0976-2833 VOL14, ISSUE 08, 2023

3.5 Ex-Vivo Studies

Cellular uptake of fluorescein isotiocyanate (FITC) loaded GNPs

Results shows that as the time increases, FITC level increases in macrophage cell lines (J774) which may be due to cellular uptake of FITC loaded mannosylated GNPs. This result shows that with rifabutin loaded mannosylated GNPs, high drug concentration can be achieved in alveolar macrophages as it can bypass the metabolism by Kupffer cells of liver (Table 12 & Fig 14).

Table 12: Cellular uptake of FITC loaded mannosylated GNPs.

S. No.	Time (hrs)	Mean FITC level
1.	1	321
2.	2	604
3.	6	630

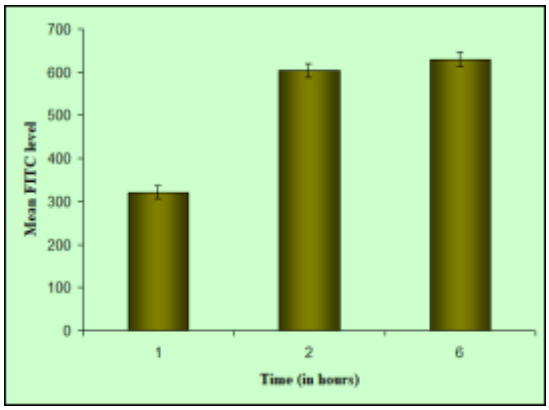

S.D. ± Mean (n=3)

Fig 14: Cellular uptake of FITC loaded mannosylated GNPs

MTT cytotoxicity assay

The mannosylated GNPs at a drug concentration of 1mg/ml showed negligible cytotoxicity in J774 cells (Fig15) possibly due to shielding of the internal cationic charges by surface hydroxyl groups of mannoses. The observed cytotoxicity of rifabutin-loaded mannosylated GNPs was much lower than that of rifabutin-loaded solid lipid nanoparticles at all concentrations. (Table 13)

ISSN: 0975-3583, 0976-2833 VOL14, ISSUE 08, 2023

Table 13 MTT cytotoxicity assay of rifabutin loaded mannosylated GNPs

Concentration(ug/ml)	Absorbance	
	Rifabutin loaded mannosylated GNPs	Rifabutin loaded GNPs
5	0.428	**0.521**
10	0.429	**0.450**
20	**0.326**	**0.369**

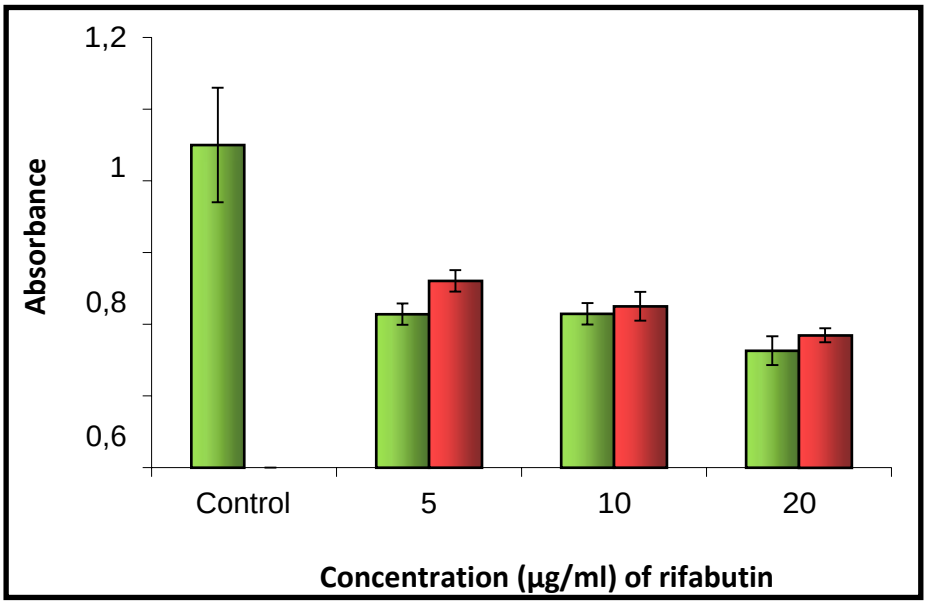

S.D. ± Mean (n=3)

Fig 15: MTT cytotoxicity assay of rifabutin loaded GNPs and MN GNPs.

Hemolytic Toxicity

The hemolytic toxicity of rifabutin and rifabutin loaded GNPs was evaluated and the percentage hemolysis on addition of GNPs formulations is shown in fig.16 with the data given in table 13. Rifabutin loaded mannosylated GNPs showed the lowest hemolytic toxicity as compared to rifabutin loaded GNPs, which might be due to the increased hydrophilicity of rifabutin loaded mannosylated GNPs. (Table 14)

Table 14- Percent hemolysis by different formulations on addition to human RBC.

ISSN: 0975-3583, 0976-2833 VOL14, ISSUE 08, 2023

Formulations	Percent Hemolysis after 1hr
Plain rifabutin solution	21.09±1.5
Rifabutin loaded GNPs	13.62±0.8
Rifabutin loaded mannosylated GNPs	10.81±0.9

S.D. ± Mean (n=3)

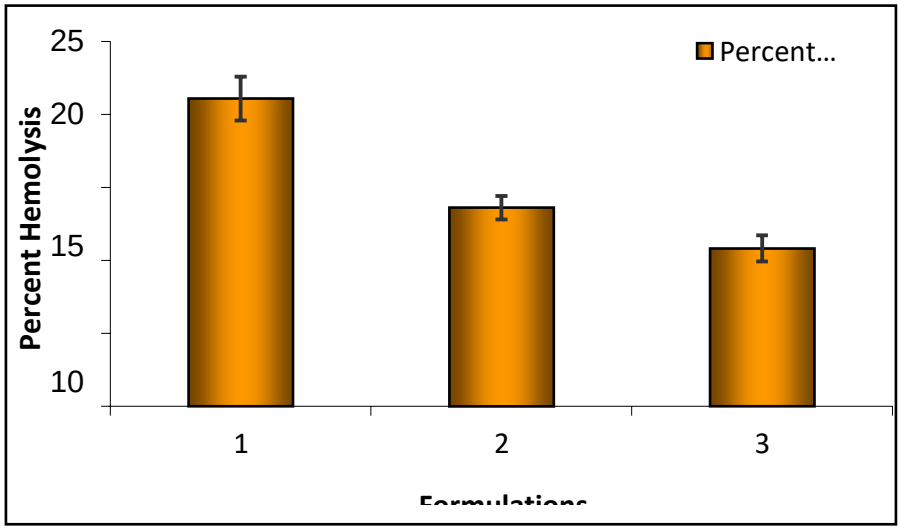

Fig.16- Percent hemolysis by 1) plain drug 2) GNPs and 3) MN GNPs formulations.

Discussion

TB is a bacterial infection that is extremely contagious and kills people all over the world. The problems with the present dosage forms of antitubercular medicines may be resolved by designing a site-specific delivery system for antitubercular drugs using surface-modified gelatin nanoparticles. The creation of rifabutin-containing gelatin nanoparticles for the treatment of tuberculosis was the aim of the current effort. Rifabutin-based nano-based medication delivery methods have not been extensively reported. In order to distribute rifabutin to alveolar tissues specifically, Nimje and colleagues [(28)] successfully created nanoparticles. The synthesis and effective mannosylation of rifabutin-loaded solid lipid nanoparticles (SLNs) were accomplished. Studies of SLNs formulations' ex vivo cellular absorption in alveolar macrophages showed that

ISSN: 0975-3583, 0976-2833 VOL14, ISSUE 08, 2023

the mannose coating significantly increased uptake by nearly six times. As an alternative, stearic acid-based SLNs have been investigated as an efficient drug delivery method for anti-tubercular medications [29-30] and proven to be a solid foundation for lowering dose frequency and enhancing patient compliance. In these present study gelatin nanoparticles were developed because Gelatin is a naturally occurring, flexible biopolymer that has a number of key applications since it is inexpensive, easily accessible, biodegradable, and biocompatible as well as having a large number of active groups. [31]

Initially the preformulation studies of refabutin was conducted, the focus of preformulation investigations is on the physicochemical concepts that are essential for every new pharmacological molecule and/or proteins/peptides. Their creation of their particular dosage form is also impacted by these characteristics, in addition to the therapeutic effectiveness. [32] The results demonstrated the sample's authenticity and purity. The maximum absorbance of the drug was found to be 275 nm using a UV spectrophotometer, which is in accordance with pharmacopoeia standards. Examining the medication's solubility in various solvents revealed that it was moderately soluble in water, sparingly soluble in ethanol, and soluble in chloroform and methanol. A capillary tube melting point apparatus was used to ascertain the drug's melting point. The melting point was found to be at about 1530 degrees Celsius, which agreed with the pharmacopoeia's listed melting point. Rifabutin was used to create a rifabutin standard curve in PBS with a pH of 7.4 using an ultraviolet spectrophotometer. The Lambert beer law was demonstrated to be followed by rifabutin in the concentration range of 2 to 20 g/ml. According to the Beer-Lambert law, there will be a linear relationship between an absorbing species' molar concentration and absorbance. It has to do with how light is absorbed and how the qualities of the medium through which the light is travelling. The drug-excipient interaction was found using infrared spectroscopy. The pharmaceutical sample's and excipient's combined IR were found to be within the recommended range. The drug sample can therefore be utilized in the formulation because there is no interaction between it and the excipients anticipated to be employed. Preparation of GNPs was carried out employing two-step desolvation method. Since the nanoparticles produced by this method have been shown to be spherical, have a small particle size, a low particle density index (PDI), and a good entrapment efficiency, it was decided to use this method for the preparation of GNPs.

ISSN: 0975-3583, 0976-2833 VOL14, ISSUE 08, 2023

Alveolar macrophages serve as the main host for MTb, allowing the pathogen to develop, reproduce, and disseminate throughout the body. As a result, selectively targeting alveolar macrophages proved a successful tactic for curing the illness. But this is possible by surface functionalizing nanocarriers with different ligands that have a particular affinity for the alveolar macrophages. Mannose, a carbohydrate ligand, possesses unique mannose receptors (MR) on macrophages, which aid in the internalization and targeted delivery of nanocarriers. [(33)] In the present study Coupling of mannoses to GNPs was done. The average particle size of mannosylated GPs was 373±23 nm. The result of zeta potential has been recorded at 11.46±0.26mV. the electrical double layer that surrounds a nanoparticle in solution and has an electrostatic potential. The zeta potential is what is used to describe this. When the zeta potential of a nanoparticle is between -10 and +10 mV, it is said to be roughly neutral, however when it is larger than +30 mV or lower than -30 mV, it is said to be strongly cationic or anionic. Zeta potential can influence a nanoparticle's propensity to permeate membranes because the majority of biological membranes have a negative charge, with cationic particles typically exhibiting increased toxicity due to rupture of the cell wall. [(34)] Percent drug loading was found to be 52.4±1.68 which was lesser than RIF loaded GNPs. The amount of drug loaded per unit weight of the nanoparticle is known as loading capacity, and it shows what proportion of the mass of the nanoparticle is made up of drug-encapsulated substance. By dividing the entire weight of the nanoparticles by the total amount of drug contained, one can get the loading capacity (LC %). Drug loading in NP varies greatly and frequently depends on the production technique. [(35)] In the present study *in vitro* drug release profiles of RIF loaded GNPs and MN-GNPs were studied using dialysis membrane. Although there is no regulatory or compendial standard, the in vitro release study is a crucial test to evaluate the safety, effectiveness, and quality of nanoparticle-based drug delivery systems. It is challenging to directly compare different systems due to the range of testing methodologies. [(36)] In our study the release behavior of RIF from the gelatin matrix showed a biphasic pattern that is characterized by an initial burst, followed by a slower sustained release. The GNP formulation showed 94.2±6.38% drug release in 120 hours, whereas the MN-GNPs showed 84.64±5.76% RIF release at the end of 120 hours. These findings were also similar to the study conducted by Saraogi G et al. [(37)]

The physical stability of gelatin nanoparticle compositions was examined for one month.

ISSN: 0975-3583, 0976-2833 VOL14, ISSUE 08, 2023

Nanoparticle stability in terms of shape is defined as the conservation of the original local structure and radius of curvature at the atomic and nanoscales as these dimensions directly impact surface free energy. The retention of nanostructures' catalytic, plasmonic, and mechanical properties is facilitated by this crucial stability descriptor. Because morphological changes affect surface facet percentages, instability occurs in this situation when surface energy declines as a result of shape changes. [(38)] In the present study all gelatin nanoparticle formulations were tested for their ability to encapsulate at various temperatures, and the results showed that formulations stored under refrigeration (4–80C) were significantly more stable than formulations stored at room temperature.

The physicochemical properties of nanoparticles, such as size, shape, and surface chemistry, as well as the used experimental settings, have an impact on the uptake of the nanoparticles by the cellular systems through a process known as endocytosis. [(39)] The xanthene dyes category includes the fluorescent dye fluorescein-5-isothiocyanate (FITC). FITC is used to label a variety of biomolecules, including oligo- and polysaccharide- rides, immunoglobulins, lectins and other proteins, peptides, nucleic acids, and nucleotides. Fluorescein-labeled annexin thus can be used to detect and quantitate the apoptotic/dead cells under microscopes or with flow cytometry. [(40)] The results of research on cellular uptake indicated that FITC levels in macrophage cell lines (J774) increase with time, which may be a result of the body absorbing FITC-loaded mannosylated GNPs. Rifabutin-loaded mannosylated GNPs were found to have significantly reduced cytotoxicity in the MTT experiment than rifabutin-loaded solid lipid nanoparticles at all doses. Rifabutin's hemolytic activity was considerably reduced when it was loaded with GNPs. Rifabutin-loaded mannosylated GNPs displayed the least hemolytic toxicity as compared to rifabutin-loaded GNPs. Therefore, MN-GNPs may be a workable and effective choice for the controlled and secure administration of RIF in tuberculosis-targeted therapy.

The MTT assay method measures the activation metabolism in a cell's mitochondrion and quantifies the impact of nanoparticles on the proliferation of the cell as a way to assess the risk of nanoparticles. In conclusion, the three-week direct colorimetric MTT assay offers a straightforward, quick, and affordable diagnostic and susceptibility test method for M. tuberculosis. The growth of bacteria in the media can be seen visually or through spectrophotometric analysis. [(41)] In the present study mannosylated GNPs at a drug concentration

ISSN: 0975-3583, 0976-2833 VOL14, ISSUE 08, 2023

of 1mg/ml showed negligible cytotoxicity in J774 cells. This result was also in accordance with the study conducted by Upadhyay et al. they reported that Rifabutin loaded alginate sealed GP are not cytotoxic upon uptake by macrophages, they performed MTT viability assay against J774A. The RB loaded GP did not show cytotoxicity to J774 cells, upon 24 h exposure up to a concentration of 80 μg/ml. [(42)]

Most NPs have hemolytic activity; however, it depends on concentration, structure, size, and shape. For instance, the amount of reactive silanol groups exposed on the surface of silica NP is directly related to the size and geometry of the NP. [(43)] In present study Rifabutin loaded mannosylated GNPs showed the lowest hemolytic toxicity as compared to rifabutin loaded GNPs. The hemolytic activity of plain rifabutin was reduced to a considerable extent when loaded in GNPs. But results for decline in hemolytic activity of rifabutin were obtained when it was present in mannosylated GNPs. This was supposed to be due to the combined effect of slow release of rifabutin and increased hydrophilicity of mannosylated GNPs.

Conclusion –

In light of the aforementioned findings, we can draw the conclusion that the proposed drug delivery method containing rifabutin gelatin nanoparticles may show to be a promising route towards the creation of an efficient TB therapy. Additionally, the capacity of this carrier to carry the medication precisely to the site of action may make it easier for the drug's inherent targeting of the infected alveolar cells. Although the exploration of GNPs containing rifabutin increased targeting is a commendable effort, more research is still required to create this carrier for futuristic drug delivery. Additionally, it is envisioned that by searching for newer bioactive, this strategy's potential field of application can be expanded.

References-

1. Dua K, Rapalli VK, Shukla SD, Singhvi G et al. multi-drug resistant Mycobacterium tuberculosis & oxidative stress complexity: Emerging need for novel drug delivery approaches. *Biomedicine & Pharmacotherapy*; 2018: 107, 1218-1229
2. Global tuberculosis report 2021. Geneva: World Health Organization; 2021. Licence: CC BY-NC-SA 3.0 IGO

ISSN: 0975-3583, 0976-2833 VOL14, ISSUE 08, 2023

3. World Health Organization (WHO), Guidelines for Treatment of Drug-Susceptible Tuberculosis and Patient Care: Essential First-Line Antituberculosis Drugs, WHO, Geneva, Switzerland 2018.
4. Raviglione MC, Harries AD, Msiska R, et al. Tuberculosis and HIV: current status in Africa. *AIDS* 1997; 11(Suppl B): S115–23
5. Adams, Kristin N., John D. Szumowski, and Lalita Ramakrishnan. "Verapamil, and its metabolite norverapamil, inhibit macrophage-induced, bacterial efflux pump-mediated tolerance to multiple anti-tubercular drugs." *The Journal of infectious diseases* 210.3 (2014): 456-466.
6. Conradie F, Diacon AH, Ngubane N, Howell P, Everitt D, Crook AM, et al. Bed aquiline, pretomanid and linezolid for treatment of extensively drug resistant, intolerant or nonresponsive multidrug resistant pulmonary tuberculosis. *N Engl J Med*. 2020;382(10):893–902.
7. Patil K, Bagade S, Bonde S, Sharma S, Saraogi G. Recent therapeutic approaches for the management of tuberculosis: Challenges and opportunities. *Biomed Pharmacotherapy*. 2018; 99: 735–45.
8. Jahagirdar PS, Gupta PK, Kulkarni SP, Devarajan PV. Intramacrophage delivery of dual drug loaded nanoparticles for effective clearance of Mycobacterium tuberculosis. *J Pharm Sci.* 2020; 109(7): 2262–70.
9. Makled S, Boraie N, Nafee N. Nanoparticle-mediated macrophage targeting-a new inhalation therapy tackling tuberculosis. *Drug Deliv Transl Res*. 2021; 11(3): 1037–55.
10. Pandit S, Roy S, Pillai J, Banerjee S. Formulation and intracellular trafficking of lipid-drug conjugate nanoparticles containing a hydrophilic antitubercular drug for improved intracellular delivery to human macrophages. *ACS Omega*. 2020; 5(9): 4433–48.
11. Alzahabi KH, Usmani O, Georgiou TK, Ryan MP, Robertson BD, Tetley TD, Porter AE. Approaches to treating tuberculosis by encapsulating metal ions and anti-mycobacterial drugs utilizing nano- and microparticle technologies. *Emerg Top Life Sci*. 2020 ;4(6):581-600.
12. Costa-Gouveia J, Aínsa JA, Brodin P, Lucía A. How can nanoparticles contribute to antituberculosis therapy? *Drug Discov Today*. 2017 ;22(3):600-607.

ISSN: 0975-3583, 0976-2833 VOL14, ISSUE 08, 2023

13. Ladaviere C, Gref R. Toward an optimized treatment of intracellular bacterial infections: input of nanoparticulate drug delivery systems. *Nanomedicine (Lond).* 2015;10(19):3033–55.
14. Rao JP, Geckeler KE. Polymer nanoparticles: preparation techniques and size-control parameters. *Prog Polym Sci*. 2011;36(7):887–913.
15. Bamrungsap S, Zhao Z, Chen T, et al. Nanotechnology in therapeutics: a focus on nanoparticles as a drug delivery system. *Nanomedicine*. 2012;7(8):1253–1271
16. Mishra B, Patel BB, Tiwari S. Colloidal nanocarriers: a review on formulation technology, types and applications toward targeted drug delivery. *Nanomedicine*. 2010;6(1):9–24
17. Chopra, H.; Mohanta, Y.K.; Rauta, P.R.; Ahmed, R.; Mahanta, S.; Mishra, P.K.; Panda, P.; Rabaan, A.A.; Alshehri, A.A.; Othman, B.; et al. An Insight into Advances in Developing Nanotechnology Based Therapeutics, Drug Delivery, Diagnostics and Vaccines: Multidimensional Applications in Tuberculosis Disease Management. *Pharmaceuticals* 2023, 16, 581.
18. Grotz, E.; Tateosian, N.; Amiano, N.; Cagel, M.; Bernabeu, E.; Chiappetta, D.A.; Moretton, M.A. Nanotechnology in Tuberculosis: State of the Art and the Challenges *Ahead. Pharm. Res*. 2018, 35, 213.
19. Azimi B, Nourpanah P, Rabiee M, Arbab S. Producing gelatin nanoparticles as delivery system for bovine serum albumin. *Iran Biomed J*. 2014;18(1):34-40.
20. Martin's Physical Pharmacy and Pharmaceutical Sciences: Physical Chemical and Biopharmaceutical Principles in the Pharmaceutical Sciences. Baltimore, MD: Lippincott *Williams & Wilkins*, 2011.